Temperature-Dependent Magnetic Circular Dichroism of Lutetium Bisphthalocyanine†

Cara L. Dunford‡ and Bryce E. Williamson*

Department of Chemistry, University of Canterbury, Private Bag 4800, Christchurch, New Zealand

Elmars Krausz

Research School of Chemistry, The Australian National University, Canberra, ACT 0200, Australia

Received: September 30, 1999; In Final Form: January 10, 2000

Magnetic circular dichroism (MCD) and absorption spectra are reported for the Q, RV, and IV band regions (6000−19000 cm^{-1}) of lutetium bisphthalocyanine in poly(methyl methacrylate) films and Ar matrixes. Weak, temperature-independent MCD of the IV band (∼7500 cm^{-1}) is consistent with its assignment to the intervalence transition of a delocalized mixed-valence system. The temperature-dependent MCD of the Q (∼15300 cm^{-1}) and RV (∼11000 cm^{-1}) bands is quantified by moment analysis and interpreted to indicate excited-state spin−orbit splittings due to weak mixing of metal and ligand π orbitals. The spectra are semiquantitatively consistent with interpretation of these bands as arising from fully allowed transitions terminating in exciton coupling states derived principally from $\pi^* \leftarrow \pi$ excitations of the individual ligands.

I. Introduction

The metallobisphthalocyanines (MPc_2) are sandwich-like complexes in which the macrocyclic ligands are staggered by 45° to give the complex D_{4d} symmetry.[1] They are of interest because of their electrochromic, semiconducting, and nonlinear optical properties.[2] Furthermore, principles developed in understanding their electronic structure and spectroscopy may be relevant to the elucidation of the roles and mechanisms of action of biologically important porphyrin-like dimers, such as the special pair of chlorophyll molecules in photosynthetic reaction centers.[3,4]

A number of optical spectroscopic studies of $LuPc_2$ have been performed.[5−14] The most detailed was conducted by VanCott et al. who measured magnetic circular dichroism (MCD) and absorption spectra of $LuPc_2$ isolated in solid Ar ($LuPc_2$/Ar).[10] Below ∼20000 cm^{-1} their spectra comprised a strong Q band, with an origin at ∼15600 cm^{-1} and sidebands to the blue, as well as weaker near-infrared features denoted the "intervalence" (IV; ∼7 500 cm^{-1}) and "red vibronic" (RV; ∼11000 cm^{-1}) bands.

Discussion of the electronic structure and transitions of $LnPc_2$ complexes rests substantially on whether the electronic states are regarded as being delocalized over both ligands. The most recent experimental evidence[9−11] supports delocalization (in agreement with conclusions for bisporphyrin analogues[3,15]) and the assignment of the IV band to the intervalence transition (Figure 1) is well established.[9−11,16,17] However the assignments of other bands are less certain.

The first theoretical attempt to interpret the spectrum of $LuPc_2$ as a delocalized system was made by Orti et al. using a molecular orbital (MO) model based on a valence effective Hamiltonian (VEH) calculation.[16] The Q band was assigned to three overlapping allowed transitions[10] arising from the excitations $e_1(\pi^*) \leftarrow a_2(\pi)$ and $e_3(\pi^*) \leftarrow b_1(\pi)$, while the RV band was assigned to the vibronically activated forbidden process $e_3(\pi^*) \leftarrow a_2(\pi)$ (Figure 1). More recently, Rousseau et al., using an extended Hückel MO calculation, gave a similar assignment for the Q band but attributed the RV band to the $a_2(\pi) \leftarrow b_1(\pi)$ intervalence excitation.[18]

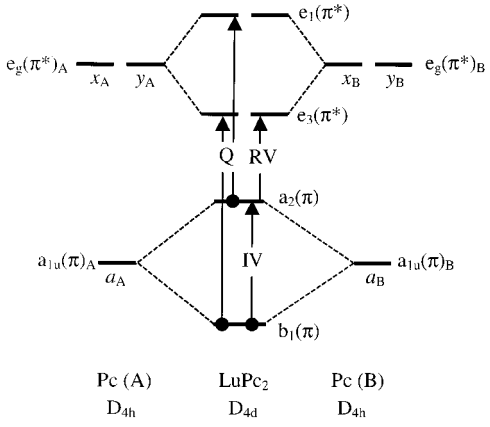

Figure 1. Frontier molecular orbitals for $LuPc_2$, indicating ligand parentage and the excitations assigned to the Q, RV, and IV bands by Orti et al. using the VEH-MO model.[16] These assignments were supported by VanCott et al.[10] Rousseau et al. assigned the $a_2(\pi) \leftarrow b_1(\pi)$ intervalence excitation to the RV band.[18]

Ishikawa et al. used a different approach, employing a configuration interaction (CI) calculation on a localized molecular orbital (LMO) basis set, essentially comprising MOs confined to each of the two ligands.[17] They concurred with the IV band assignment, but attributed all other bands below ∼20000 cm^{-1} to allowed $^2E_1 \leftarrow {}^2A_2$ transitions terminating in excited states described as admixtures of delocalized "exciton coupling" and "charge resonance" states of $e_g(\pi^*) \leftarrow a_{1u}(\pi)$ (in D_{4h}) ligand parentage.[17,19] Their calculated spectrum showed a single, strong transition near 15700 cm^{-1} with weaker bands to both the red and blue.

† Part of the special issue "Marilyn Jacox Festschrift".

* Corresponding author. E-mail: B.Williamson@chem.canterbury.ac.nz. Fax: ++ 64 3 364 2110.

‡ Present address: Department of Chemistry, University of Western Australia, Nedlands, Perth, WA 6907, Australia.

10.1021/jp993497b CCC: $19.00
Published on Web 03/07/2000

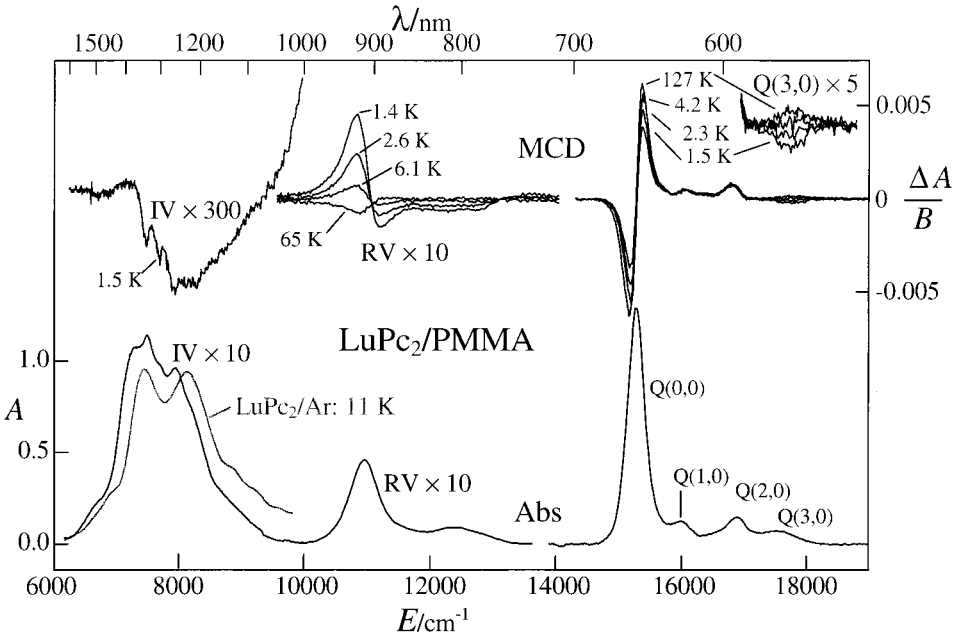

Figure 2. Temperature-dependent MCD (ΔA per tesla; top) and 1.5 K absorption (A; bottom) spectra of $LuPc_2$/PMMA. The near-infrared absorption bands (<14000 cm^{-1}) are amplified by a factor of 10. The RV and IV band MCD are amplified by factors of 10 and 300, respectively. The 11 K absorption spectrum of the $LuPc_2$/Ar IV band is reproduced from ref 11.

In an attempt to discriminate experimentally between these assignments, VanCott et al. came down in favor of Orti et al.'s VEH-MO model, essentially on the basis of two spectroscopic observations.[10] First, they interpreted structure in the Q band of $LuPc_2$/Ar to indicate the presence of more than one strong transition. Second, they found that the sign of the RV-band MCD changed on going from $CDCl_3$ solution at room temperature to an Ar matrix at ~7 K, behavior which they believed to be incompatible with assignment of the band to an allowed transition.

In this work, absorption and temperature-dependent MCD spectra are reported over the range 6000−19000 cm^{-1} for $LuPc_2$/PMMA (PMMA = poly(methyl methacrylate)) and $LuPc_2$/Ar. The results have been used to reassess the relative merits of the rival assignments for the Q and RV bands.

II. Experimental Section

PMMA films were produced by dissolving $LuPc_2$ (synthesized by T. C. VanCott[10]) and the polymer in chloroform, then allowing the solvent to evaporate overnight. Ar matrixes were formed by co-depositing $LuPc_2$ (sublimed from a Knudsen cell at $T \approx 600$ K) with Ar onto a cold ($T \lesssim 20$ K) c-cut sapphire window. Deposition times were typically 20 min, using an Ar flow rate of ~2 mmol h^{-1}.

MCD and double-beam absorption spectra of the Q and RV bands of $LuPc_2$/Ar and $LuPc_2$/PMMA were measured at the University of Canterbury by using a double-beam spectrometer in conjunction with Hamamatsu R376 and R316 photomultiplier tubes.[20,21] Near-infrared spectra of $LuPc_2$/PMMA were measured at the Australian National University by using a single-beam spectrometer and a liquid-N_2-cooled InSb detector.[22] Spectral resolution was ~0.2 nm.

Preliminary measurements and annealing studies of matrix-isolated samples were conducted by using a closed-cycle He refrigerator (APD Cryogenics) placed between the poles of an Alpha Magnetics 4800 electromagnet.[20,21] Temperature and magnetic field dependence studies were performed by using an Oxford Instruments SM4 cryomagnet,[14,23] which allows stronger magnetic fields, lower temperatures, and more precise thermometry.

III. Results

The 1.5 K absorption (A) and temperature-dependent MCD (ΔA) spectra of $LuPc_2$/PMMA shown in Figure 2 are composites, from two samples, of data normalized to the give the same integrated absorbance for the temperature-independent RV band. ΔA is the difference between the absorbance of left (A_L) and right (A_R) circularly polarized light by a sample in the presence of a longitudinal magnetic field of inductance B, while A is the corresponding average:[24]

$$\Delta A = A_L - A_R \quad (1)$$

$$A = (A_L + A_R)/2 \quad (2)$$

The Q band spectra (~14500−17500 cm^{-1}) are very similar to those of both $LuPc_2$[9] and transition-metal monophthalocyanines (MPcs)[25] in solution. The bands Q(0,0), Q(1,0), and Q(2,0) are labeled according to the established convention for MPcs.[25] The IV, RV, and Q(3,0) bands are not observed in MPc spectra and their nomenclature follows VanCott et al.[10]

The MCD of Q(0,0) has the dispersion of a positive A term (a temperature-independent derivative-shaped feature with the negative lobe at lower energy) but exhibits temperature dependence that indicates the presence of C terms.[24] The MCD of the Q(3,0) band is positive at high temperature but becomes negative below ~4 K.

The near-infrared bands are much weaker than Q(0,0) and have been amplified in Figure 2. The absorption and high-temperature ($T \gtrsim 50$ K) MCD of the RV band are similar to earlier solution-phase spectra.[9,10] The MCD has the appearance of an asymmetric positive A term at high temperatures but also shows striking temperature dependence with a reversal of sign at $T \approx 10$ K. At low temperatures ($T < 10$ K), the spectra resemble those reported by VanCott et al. for $LuPc_2$/Ar at ~7 K.[10]

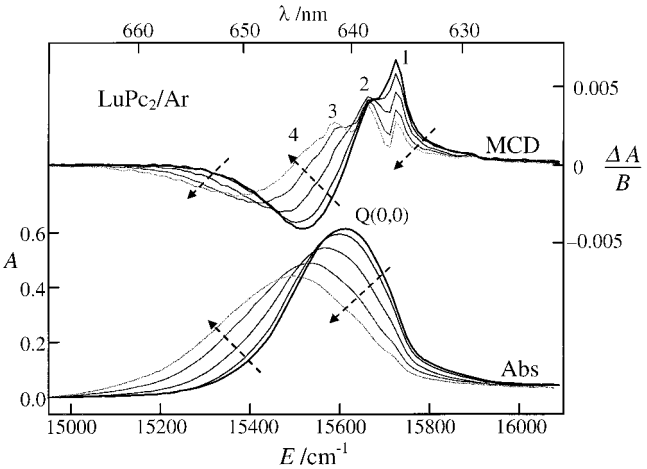

Figure 3. The effect of annealing on the Q(0,0) band structure of $LuPc_2$/Ar. The pre-anneal spectrum ($T \approx 15$ K) is plotted in black. The results of progressive anneals for 10−15 min at ∼20, 28, 34, and 38 K are shown in lighter shades. Arrows indicate the direction of change with annealing.

The 1.5 K IV band absorption spectrum is similar to the 11 K spectrum of $LuPc_2$/Ar (shaded curve Figure 2),[10,11] except for a ∼200 cm^{-1} red shift and slightly more complicated structure. The IV band MCD (amplified by 300 in Figure 2), which has not been reported previously, is extremely weak and shows no perceptible temperature dependence.

The $LuPc_2$/Ar spectra differ only slightly from those for $LuPc_2$/PMMA and are not reproduced here.[14] However, some $LuPc_2$/Ar samples prepared using the closed-cycle refrigerator/electromagnet system showed a substantially sharper Q(0,0) band with a blue-shifted absorption maximum and a very similar appearance to that reported by VanCott et al.[10] As demonstrated in Figure 3, the difference can be attributed to the degree of annealing. The dark spectrum was obtained from the unannealed matrix deposited at ∼15 K, while the others were measured at ∼15 K after progressive annealing for 10−15 min at ∼20, 28, 34, and 38 K. As annealing proceeds, the band becomes broader and shifts to the red. The intensity of the positive MCD lobe is transferred from a sharp high-energy band (labeled 1) to a series of lower energy bands (labeled 2−4).

The band intensities are quantified by spectroscopic moments defined by[24]

$$\mathbf{A}_n = \int (A/E)(E - \bar{E})^n \, dE \qquad (3a)$$

$$\mathbf{M}_n = \int (\Delta A/E)(E - \bar{E})^n \, dE \qquad (3b)$$

E is the wavenumber (cm^{-1}), and $\bar{E}$ is the absorption band barycenter defined by $\mathbf{A}_1 = 0$. $\mathbf{A}_0$ is used to measure the absorption intensity, while $\mathbf{M}_1$ is used to measure the intensity of the A-term-like MCD features.

Moment analysis of the data presented in Figure 3 shows that the Q(0,0) band barycenter for $LuPc_2$/Ar shifts from 15614 to 15500 cm^{-1} with annealing. However, $\mathbf{M}_1$ and $\mathbf{A}_0$ are unchanged, giving $\mathbf{M}_1/\mu_B B\mathbf{A}_0 = 2.3 \pm 0.2$, in close agreement with the value of 2.6 obtained for $LuPc_2$/Ar by VanCott et al.[10] This invariance indicates that the changes in the appearance of the spectrum are not accompanied by significant changes of the electronic angular momenta or spin−orbit interactions in the excited state. All of these spectra clearly come from the same chemical species whose physical environment is changing. However, to circumvent any suspicions about the effect of annealing and to counter uncertainties about the degree of preferential orientation of guest molecules in cryogenic matrixes, the analyses in the following sections are restricted to $LuPc_2$/PMMA.

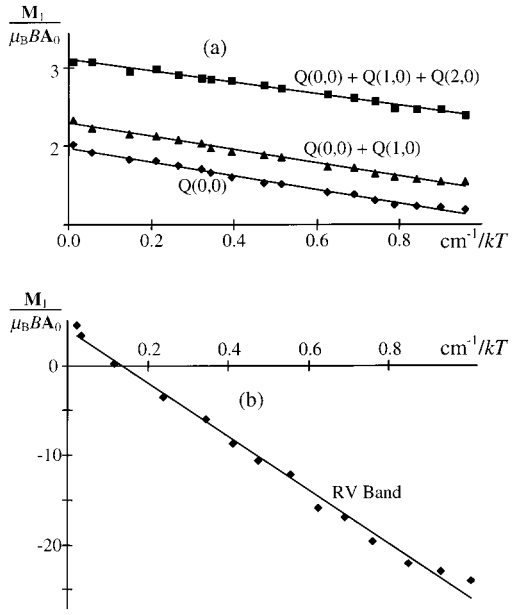

Figure 4. Temperature-dependent moment analysis plots for the spectra of $LuPc_2$/PMMA. (a) The Q band region over three integration ranges. The slopes are the same within experimental error. (b) The RV band region. The expanded ordinate scale in comparison with (a) reflects a stronger MCD temperature dependence.

Spectroscopic moments are most amenable to theoretical interpretation when integration is carried over the entire envelope of a transition, including all vibrational overtones but excluding contributions from other electronic transitions. This presents difficulties in the case of the Q band region of $LuPc_2$. Apart from the possibility that it may encompass three separate Q transitions,[10] the Q(2,0)[10,26,27] and Q(3,0)[10] bands are also believed to contain contributions from other electronic excitations. An illustration of the problem is presented in Figure 4a, where $\mathbf{M}_1/\mu_B B\mathbf{A}_0$ values obtained using a variety of integration ranges are plotted against $1/kT$ (k is Boltzmann's constant). The ordinate intercept is strongly dependent on the range of integration, but fortunately, and of importance to the analysis that follows, the effect on the slope is much weaker. After analyzing the data from a number of samples, we determine that slope to be $\mathbf{M}_1 kT/\mu_B B\mathbf{A}_0 = -0.79 \pm 0.10$ cm^{-1}.

The plot of $\mathbf{M}_1/\mu_B B\mathbf{A}_0$ against $1/kT$ for the RV region of $LuPc_2$/PMMA (Figure 4b) has a slope of -30 ± 4 cm^{-1} and an intercept of 3.8 ± 1.1.

IV. Discussion

$LuPc_2$ is and odd-electron system in which the Lu^{3+} ion has a formal closed-shell [Xe]$4f^{14}$ configuration and the average charge on each ligand is −3/2. The ground-state is $^2A_2$ with the unpaired electron residing in the $a_2(\pi)$ HOMO comprising the antibonding combination of $a_{1u}(\pi)$ orbitals of the two Pc rings (Figure 1).[10]

The allowed transitions from the ground state are $^2B_1 \leftarrow {}^2A_2$ (z polarized) and $^2E_1 \leftarrow {}^2A_2$ (x, y polarized). The MCD of the former comprises only B terms, which should be weak and temperature independent, requirements that preclude the possibility that the RV band is due to the $a_2(\pi) \leftarrow b_1(\pi)$ intervalence excitation.[18] The orbital degeneracy of $^2E_1$ gives temperature-independent A terms,[24] while the combination of ground-state spin degeneracy and excited-state spin−orbit (SO) splitting

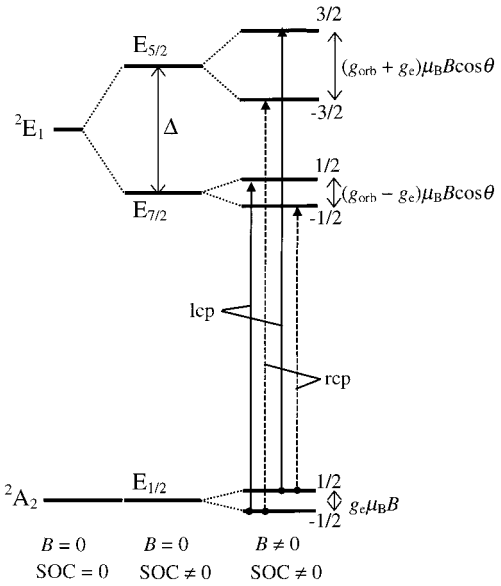

Figure 5. Energy level diagram, including the effects of spin−orbit coupling and Zeeman interactions, for a $^2E_1 \leftarrow {}^2A_2$ transition in D_{4d} symmetry. Full and dashed lines indicate right and left circularly polarized transitions, respectively. Parameters and labels are defined in the text.

cause a temperature-dependent pseudo-*A* term (comprising a pair of overlapping, oppositely signed *C* terms), the sign of which depends on the relative energies of the SO levels.[14,23]

IV Band. An inability to detect the MCD associated with the IV band of a room-temperature $LuPc_2/CDCl_3$ solution has been previously cited as evidence for assigning the band to a *z*-polarized transition.[10] The weak, temperature-independent, negative *B* term associated with the IV band in Figure 2 confirms this conclusion and thereby reinforces the assignment to the $^2B_1 \leftarrow {}^2A_2$ intervalence transition.

The different profiles of the absorption and MCD are indicative of vibronic activity, an inherent feature of intervalence transitions of mixed-valence systems.[11] A detailed analysis of this phenomenon is beyond the scope of this report, but simple considerations indicate that the *B* term intensities of individual vibronic components are determined by the details of vibronic coupling and are not simply proportional to the absorbance. The weighting of the MCD to the blue of the absorbance indicates that the *B* terms are principally a result of Zeeman coupling of the excited state with higher-lying states, probably those associated with the IV and Q bands. Vibronic levels toward the blue end of the band envelope are closer to the states with which they couple and consequently have stronger *B* terms.

Moment Analysis of $^2E_1 \leftarrow {}^2A_2$ in D_{4d} Symmetry. The RV and Q bands have MCD dispersion and temperature dependence that are clearly in accord with $^2E_1 \leftarrow {}^2A_2$ transitions. For the RV band, the excited-state label may reflect *vibronic* rather than pure electronic symmetry,[10,16] but the same general analysis applies except for a possible reversal in the sign of the *A* term depending of the symmetry of the activating vibration.[10]

The treatment of $^2E_1 \leftarrow {}^2A_2$ for $LuPc_2$ is analogous to $^2E_u \leftarrow {}^2B_{1g}$ for CuPc.[23,28] The relevant energy level diagram is shown in Figure 5. At zero magnetic field, the excited term is split into doubly degenerate $E_{5/2}$ and $E_{7/2}$ levels, separated by

$$\Delta = \bar{E}_{5/2} - \bar{E}_{7/2} \tag{4}$$

where $\bar{E}_t$ is the band barycenter for the transition to the E_t level. An external magnetic field at angle θ with respect to the molecular 4-fold axis gives the Zeeman splittings shown at the right of the figure, where g_{orb} is a measure of the excited-state orbital angular momentum.

Figure 5 also shows the allowed Zeeman transitions and their polarizations. They have equal dipole strengths, so their relative intensities are determined by the Boltzmann populations of the ground-state Zeeman levels from which they originate. As a consequence, $\mathbf{M}_1$ comprises a temperature-independent part (*A* term) whose magnitude is determined by g_{orb}, and a temperature-dependent part (pseudo-*A* term) whose intensity depends on Δ.[14,23] In the linear limit ($\mu_B B \ll kT$), the relationship is

$$\mathbf{M}_1/\mu_B B\mathbf{A}_0 = (g_{orb} - \Delta/kT)/2 \tag{5}$$

where the factor of 1/2 pertains to an ensemble of randomly oriented molecules.

Equation 5 and the data in Figure 4b yield $\Delta^{RV} = 60 \pm 8$ cm^{-1} and $g_{orb}^{RV} = 7.6 \pm 2.2$, while the average slope of the plots in Figure 4a gives $\Delta^{Q} = 1.6 \pm 0.2$ cm^{-1}. Since the Q(2,0) band is believed to contain a contribution from another transition,[10,26,27] the g_{orb} values obtained by its inclusion and exclusion should bracket the "true" value for the Q excited state; hence, we estimate $g_{orb}^{Q} = 5.4 \pm 2.0$.

In summary, the effective g_{orb} values of the Q and RV bands are the same within experimental error. The effective zero-field splittings have the same sign ($E_{5/2}$ level at higher energy) but that for the RV state is larger by a factor of ~40.

The Origin of Δ. The major contribution to Δ for a ^2E term would normally arise from SO splitting. McClure has shown that SO coupling in planar $\pi(p_z)$ systems (such as free-base porphyrins) must be weak,[29] while the spatial separation of the two Pc rings should preclude significant inter-ring SO interactions in $LuPc_2$. However, the presence of a metal ion can introduce contributions through π−metal mixing,[23,30] which are most conveniently considered within the framework of a delocalized MO model; e_1 ligand MOs can mix with metal p and f orbitals, while e_3 can mix with d and f.[31] Rousseau et al. considered π−metal overlap in their extended Hückel calculation.[18] They ignored f orbitals (due to contraction) and, with regard to the frontier orbitals of Figure 1, restricted themselves the qualitative statements to the effect that orbital overlap is very weak. However, the SO coupling constants of the lanthanide ions are very large,[32,33] so weak mixing does not necessarily preclude significant splittings.

We define SO parameters for the (mixed π−metal) e_1 and e_3 orbitals by

$$Z_1 = i\langle e_1 x|\sum_k \xi_{e_1}(k) l_z(k)\ |e_1 y\rangle \tag{6a}$$

$$Z_3 = i\langle e_3 \eta|\sum_k \xi_{e_3}(k) l_z(k)|e_3 \xi\rangle \tag{6b}$$

where $l_z(k)$ is the *z*-component one-electron operator for the orbital angular momentum about nucleus *k*, $\xi_\phi(k)$ is the corresponding SO coupling coefficient for an electron in orbital ϕ, and the sum is carried over all nuclei. In the absence of the π−metal mixing coefficients, these matrix elements cannot be evaluated. Moreover, since Lu^{3+} is a closed-shell ion, its SO coupling constants are not known. However, estimates obtained by extrapolation of data for other lanthanide ions[32,33] suggest that values of $Z \approx 60$ cm^{-1} are possible with metal orbital contributions of $\lesssim$1%.

Having discussed the general treatment of a $^2E \leftarrow {}^2A_2$ transition in D_{4d} symmetry, we now relate it to the proposed

models. For convenience, we refer to the one devised by Orti at al.[16] and supported VanCott et al.[10] as the VEH-MO model and the one due to Ishikawa et al.[17] as the CI-LMO model.

VEH-MO Model.[10,16] First we consider the transitions taken to be responsible for the Q band (Figure 1). The $e_3(\pi^*) \leftarrow b_1(\pi)$ excitation yields a $^4E_1$ term as well as two $^2E_1$ terms that VanCott et al.[10] distinguished by the spins of the unexcited $b_1(\pi)$ and $a_2(\pi)$ electrons. We denote the term in which these spins form a singlet by $^2E_1^{Q1}$, and the one in which they form a triplet by $^2E_1^{Q3}$. The $e_1(\pi^*) \leftarrow a_2(\pi^*)$ excitation gives just one doublet term denoted $^2E_1^{Q2}$.

The configurational wave functions for the $^2E_1^Q$ states are given by VanCott et al., along with treatments of dipole strengths and excited-state orbital angular momenta.[10] Neglecting CI and overlap with the metal or between orbitals on different ligands, their results yields absorption moments

$$\mathbf{A}_0^{Q1}:\mathbf{A}_0^{Q2}:\mathbf{A}_0^{Q3} = 1:2:3 \tag{7}$$

and indicate that the three $^2E_1$ excited terms shared the same g_{orb} value,

$$g_{orb}^{Q} = 2i\langle e_g x|l_z|e_g y\rangle^{D_{4h}} \tag{8}$$

In eq 8, l_z is the component of the one-electron orbital angular momentum operator about the molecular symmetry axis and the subscript on the right indicates that the matrix element pertains to a single Pc ligand with effective D_{4h} symmetry.

The SO splittings of the $^2E_1^Q$ terms are readily determined from VanCott et al.'s wave functions[10] to be

$$\Delta^{Q2} = Z_1 \tag{9a}$$

$$\Delta^{Q1} = -3\Delta^{Q3} = Z_3 \tag{9b}$$

However, since the three transitions are taken to be unresolved within the Q band envelope, only an effective zero-field splitting, Δ^Q, can be determined experimentally. $\mathbf{A}_0$ and $\mathbf{M}_1$ are additive, so Δ^Q is just the weighted sum of the individual values,

$$\Delta^{Q} = \frac{\sum \mathbf{A}_0^{Qi}\Delta^{Qi}}{\sum \mathbf{A}_0^{Qi}} = Z_1/3 \tag{10}$$

In other words, assuming the VEH-MO model, the MCD temperature dependence of the Q band reflects the zero-field splitting of the $^2E_1^{Q2} \leftarrow {}^2A_2$ transition.

In the VEH-MO model the RV band constitutes a single, formally forbidden $^2E_3 \leftarrow {}^2A_2$ transition, which gains intensity via vibronic coupling involving modes of b_1, b_2, or e_2 symmetry.[10] However, the magnitudes of g_{orb}^{RV} and Δ^{RV} are determined entirely by the electronic state. The required wave functions involve a single unpaired e_3 electron, for which straightforward evaluation gives

$$g_{orb}^{RV} = g_{orb}^{Q} \tag{11}$$

$$\Delta^{RV} = Z_3 \tag{12}$$

CI-LMO Model.[17] The relevant configurational basis states of the CI-LMO model are given as linear combinations of Slater determinants in Table 1. The $^2E_1$ terms are classified according to their accessibility by one-electron excitation from the ground state.[17] The charge resonance ($^2E_1^{CR}$) states require interligand charge-transfer excitations. The three exciton coupling terms are reached by intraligand excitations and are distinguished by the spin multiplicity of the excited ligand. If the local excited state is a spin singlet or triplet, the overall (doublet) term is referred to as a singdoublet or tripdoublet and denoted by a superscript S or T. If the doublet spin is determined entirely by the state of the excited ligand the term is referred to as a doublet and denoted by superscript D.

TABLE 1: Configurational Basis States for the CI-LMO Model of Ishikawa et al.[17]

configurational basis states[a]	Slater determinants[b]	Δ/Z[c]
$\|^2A_2 \pm 1/2\rangle$	$2^{-1/2}(\|a_A^+ a_A^- a_B^{\pm}\rangle - \|a_A^{\pm} a_B^+ a_B^-\rangle)$	0
$\|^2E_1^T\rho \pm 1/2\rangle$	$12^{-1/2}(2\|\rho_A^{\pm} a_A^{\pm} a_B^{\mp}\rangle - \|\rho_A^+ a_A^- a_B^{\pm}\rangle - \|\rho_A^- a_A^+ a_B^{\pm} - 2\|a_A^+ \rho_B^{\pm} a_B^{\pm} + \|a_A^{\pm} \rho_B^+ a_B^-\rangle + \|a_A^{\pm} \rho_B^- a_A^+\rangle)$	2/3
$\|^2E_1^D\rho \pm 1/2\rangle$	$2^{-1/2}(\|a_A^+ a_A^- \rho_B^{\pm}\rangle - \|\rho_A^{\pm} a_B^+ a_B^-\rangle)$	1
$\|^2E_1^S\rho \pm 1/2\rangle$	$2^{-1}(\|\rho_A^+ a_A^- a_B^{\pm}\rangle - \|\rho_A^- a_A^+ a_B^{\pm}\rangle - \|a_A^{\pm} \rho_B^+ a_B^-\rangle + \|a_A^{\pm} \rho_B^- a_B^+\rangle)$	0
$\|^2E_1^{CR}\rho \pm 1/2\rangle$	$2^{-1/2}(\|a_A^+ a_A^- \rho_A^{\pm}\rangle - \|\rho_B^{\pm} a_B^+ a_B^-\rangle)$	1

[a] ρ is the orbital partner label of the E_1 irrep in the D_{4d} point group. Labels $\pm 1/2$ designate spin states. Subscripts T, D, S, and CR are defined in the text. [b] Kets are Slater determinants in terms of localized spin−orbitals. Ligands A and B are indicated by subscripts; a_{1u} orbitals are represented by a; e_g orbitals are represented by the partner label ρ, referenced to the D_{4d} molecular axes; spin states $m_s = \pm 1/2$ are indicated by superscripts $+/-$. [c] Δ and Z are defined by eqs 4 and 13, respectively.

TABLE 2: CI States for the CI-LMO Model of Ishikawa et al.[17] [a]

CI states	configurational basis states	E /10^3 cm^{-1}	Δ/Z
$\|1^2E_1\,\rho \pm 1/2\rangle$	$0.880\,\|^2E_1^T\rho \pm 1/2\rangle - 0.400\,\|^2E_1^D\rho \pm 1/2\rangle + ...$	6.6	0.7
$\|2^2E_1\,\rho \pm 1/2\rangle$	$0.757\,\|^2E_1^D\rho \pm 1/2\rangle - 0.561\|^2E_1^{CR}\rho \pm 1/2\rangle + ...$	14.0	1.0
$\|3^2E_1\,\rho \pm 1/2\rangle$	$0.843\,\|^2E_1^S\rho \pm 1/2\rangle + 0.304\|^2E_1^{CR}\rho \pm 1/2\rangle + ...$	15.7	0.1
$\|4^2E_1\,\rho \pm 1/2\rangle$	$0.748\,\|^2E_1^{CR}\rho \pm 1/2\rangle + 0.400\,\|^2E_1^S\rho \pm 1/2\rangle + ...$	22.6	0.7

[a] See footnotes to Table 1 for definitions.

First-order SO splittings are presented in the rightmost column of Table 1 in terms of SO parameter Z, which can be related to those in eqs 6 by expanding the MOs as LMOs to give

$$Z = (Z_1 + Z_3)/2 \tag{13}$$

The absence of SO splitting for the $^2E_1^S$ term is a consequence of spin-singlet character of the excited ligand in each determinant.

Transitions to the charge resonance and tripdoublet states are formally forbidden but gain intensity through excited-state CI mixing with the doublet and singdoublet. The CI states determined by Ishikawa et al., numbered 1 to 4 in order of ascending energy, are given in Table 2 along with their calculated energies. On the basis of these energies and the calculated intensities, the RV and Q bands were respectively assigned to $2^2E_1 \leftarrow {}^2A_2$ and $3^2E_1 \leftarrow {}^2A_2$.[17]

Also listed in Table 2 are first-order SO splittings estimated by using Table 1 and the incomplete set of mixing coefficients provided by Ishikawa et al.[17] Accordingly, the CI-LMO model predicts

$$\Delta^{RV} \approx 10\Delta^{Q} \approx Z \tag{14}$$

All of the $^2E_1$ states listed in Tables 1 and 2 have the same orbital angular momentum and hence the predicted g_{orb} values are the same as those for the VEH-MO model and given by eqs 8 and 11.

Comparison of Theory with Experiment. Here, the predictions of the VEH-MO[16] and CI-LMO[17] models are compared with the experimental results, noting that neither of the theoretical calculations is sufficiently sophisticated to expect precise agreement with experiment.

The CI-LMO model predicts relative Q- and RV-band energies and intensities in semiquantitative agreement with the experimental absorption spectra.[17] The VEH-MO model is qualitative about both, with the RV-band intensity depending on the mechanism and strength of vibronic coupling.[10,16]

The (temperature-independent) A terms of both the Q and RV bands are positive and moment analysis gives $g_{orb}^{RV} \approx g_{orb}^{Q}$ within experimental uncertainty. The theoretical models concur about the latter result. However, whereas the CI-LMO model predicts positive A terms, the VEH-MO model is ambiguous about the sign for the RV band; a positive A term requires activating modes of e_g rather than b_1 or b_2 symmetry.[10]

The CI-LMO model predicts $\Delta^{RV}/\Delta^{Q} \approx 10$, independent of the individual values of Z_1 or Z_3 and in acceptable agreement with the experimental ratio of ~40. The VEH-MO model predicts $\Delta^{RV}/\Delta^{Q} \approx Z_3/Z_1$ but provides no information about the value of this ratio.

To this point the CI-LMO model is to be preferred on the basis that it provides semiquantitatively correct predictions, whereas the VEH-MO model is qualitative and vague in comparison. We therefore revisit the observations that led VanCott et al. to favor the latter.[10]

VanCott et al. supported the assignment of the RV band to a formally forbidden transition on the basis of an inversion of MCD attributed to a dependence of the vibronic activating mechanism on the nature host medium.[10] Our analysis shows that the inversion is a temperature-dependent consequence of ground-state spin degeneracy and excited-state SO splitting and is independent of the host. Although this explanation does not exclude the possibility of a vibronic assignment, it negates the view that the MCD behavior *demands* a vibronic assignment. Two other pieces of information militate more directly against the VEH-MO assignment. First, the RV band absorbance does not exhibit the temperature dependence expected of a vibronically activated transition.[34] Second, Markovitsi et al. report that the band disappears on reduction but is retained on oxidation,[7] exactly the opposite of the expectation for the $e_3(\pi^*) \leftarrow a_2(\pi)$ excitation (Figure 1).

VanCott et al. observed structure in the absorption and MCD of the Q band of $LuPc_2$/Ar, which they attributed to the near coincidence of three transitions within the band envelope (fwhm ~100 cm^{-1}),[10] in agreement with the VEH-MO model but contradictory to the CI-LMO prediction of one transition. Their conclusion requires accidentally equal $a_2(\pi)-b_1(\pi)$ and $e_1(\pi^*)-e_3(\pi)$ orbital separations and very weak CI between the excited states, both of which seem improbable. In this work, we find that the Q band structure depends on deposition conditions and can be modified by annealing (Figure 3). These observations are more compatible with a single transition (in accordance with the CI-LMO model) and the existence of several matrix sites.

The weight of this evidence clearly supports the CI-LMO model of Ishikawa et al.[17] Regarding the Q, RV, and IV bands, it predicts the correct number of transitions with the correct MCD dispersion and temperature dependence at semiquantitatively correct energies and intensities, without recourse to forbidden processes. Its apparent conflicts with experimental results have been resolved by following the MCD over a broad temperature range and by studying the annealing behavior of $LuPc_2$/Ar.

V. Conclusion

The observation of weak, temperature-independent MCD associated with the IV band of $LuPc_2$ bolsters the already compelling case for assigning the band to the $^2B_1 \leftarrow {}^2A_2$ intervalence transition. The dispersion and temperature dependence of the Q and RV band MCD spectra are consistent with allowed $^2E_1 \leftarrow {}^2A_2$ transitions to excited states that carry a small amount of metal ion character.

The accumulated evidence supports the CI-LMO calculation of Ishikawa et al.[17] as the best current model for the electronic spectroscopy of $LuPc_2$. The Q and RV bands are assigned to allowed transitions to exciton coupling states, essentially antisymmetric linear combinations of localized $e_g(\pi^*) \leftarrow a_{2u}(\pi)$ Pc excitations. Accordingly, the term "red vibronic band" is probably a misnomer and if the acronym RV is to be retained, the description "red valence" may be more appropriate. The specific CI-LMO assignments of the Q and RV bands, to transitions of predominantly singdoublet and doublet character, respectively (Table 2), also suggest an elegant rationale for the resemblance of the $LuPc_2$ spectrum to a superposition of those for neutral MPc and its π radical cation.[7-9,17] The singdoublet correlates with the Q transition of MPc, while the doublet correlates with the Q transition of $MPc^{\bullet+}$.[17]

The CI-LMO model predicts two further weakly allowed transitions of $e_g(\pi^*) \leftarrow a_{2u}(\pi)$ ligand parentage. The $4^2E_1 \leftarrow {}^2A_2$ transition, essentially the charge resonance transition, is calculated to lie to the blue of the Q band.[17] A likely candidate is the Q(3,0) band near 17500 cm^{-1}, which has been attributed to a separate electronic transition.[10] Although its weakness and strong overlap with Q(2,0) preclude a detailed analysis, its MCD temperature dependence is qualitatively consistent with such an assignment. We could find no evidence for $1^2E_1 \leftarrow {}^2A_2$ (principally the tripdoublet transition), which is predicted to lie between the IV and RV bands.[17]

We now return our attention to theoretical calculations. First, expansion of the delocalized MOs as linear combinations of LMOs shows that the configurational bases for the models are related by unitary transformation. They should therefore yield similar results when carried to the same computational level. The fact that they do not can almost certainly be attributed to the inclusion of CI in the calculation of Ishikawa et al.[17] and its absence from the others.[16,18] It would therefore be interesting, and perhaps informative, to see the results of a delocalized MO treatment that includes CI. Second, the temperature dependence of the MCD is ascribed here to metal ion contributions to the π^* orbitals, a supposition that should be tested by theoretical calculations, perhaps using density functional theory.

Finally, we note that preliminary spectral hole-burning studies of the Q band of $LuPc_2$/Ar[13] have more recently been extended to $LuPc_2$/PMMA with some interesting results. We intend to apply this technique to the IV band in the future.

Acknowledgment. We thank Dr. T. C. VanCott and Professor P. N. Schatz for providing the samples of $LuPc_2$.

References and Notes

(1) Paillaud, J. L.; Drillon, M.; De Cian, A.; Fischer, J.; Weiss, R.; Villeneuve, G. *Phys. Rev. Lett.* **1991**, *67*, 244−247.

(2) VanCott, T. C.; Gasyna, Z.; Schatz, P. N.; Boyle, M. E. *J. Phys. Chem.* **1995**, *99*, 4820−4830 and references therein.

(3) Donohoe, R. J.; Duchowski, J. K.; Bocian, D. F. *J. Am. Chem. Soc.* **1988**, *110*, 6119−6124.
(4) Gasyna, Z.; Schatz, P. N. *J. Phys. Chem.* **1996**, *100*, 1445−1448.
(5) De Cian, A.; Moussavi, M.; Fischer, J.; Weiss, R. *Inorg. Chem.* **1985**, *24*, 3162−3167.
(6) Burkov, V. I.; Talanina, I. B.; Mokshin, V. M.; Tomilova, L. G.; Lukyanets, E. A. *Opt. Spectrosc.* **1986**, *61*, 493−496.
(7) Markovitsi, D.; Tran-Thi, T. H.; Even, R.; Simon, J. *Chem. Phys. Lett.* **1987**, *137*, 107−112.
(8) Tran-Thi, T. H.; Markovitsi, D.; Even, R.; Simon, J. *Chem. Phys. Lett.* **1987**, *139*, 207−211.
(9) Ishikawa, N.; Ohno, O.; Kaizu, Y. *Chem. Phys. Lett.* **1991**, *180*, 51−56.
(10) VanCott, T. C.; Gasyna, Z.; Schatz, P. N. *J. Phys. Chem.* **1995**, *99*, 4820−4830.
(11) Gasyna, Z.; Schatz, P. N.; Boyle, M. E. *J. Phys. Chem.* **1995**, *99*, 10159−10165.
(12) Ostendorp, G.; Homborg, H. *Z. Anorg. Alleg. Chem* **1996**, *622*, 1222−1230.
(13) Krausz, E.; Riesen, H.; Schatz, P. N.; Gasyna, Z.; Dunford, C. L.; Williamson, B. E. *J. Lumin.* **1996**, *66/67*, 19−24.
(14) Dunford, C. L. Ph.D. Dissertation, University of Canterbury, Christchurch, 1997.
(15) Duchowski, J. K.; Bocian, D. F. *J. Am. Chem. Soc.* **1990**, *112*, 3312−3318.
(16) Orti, E.; Bredas, J. L.; Clarisse, C. *J. Chem. Phys.* **1990**, *92*, 1228−1235.
(17) Ishikawa, N.; Ohno, O.; Kaizu, Y. *J. Phys. Chem.* **1993**, *97*, 1004−1010.
(18) Rousseau, R.; Aroca, R.; Rodriguez-Mendez, M. L. *J. Mol. Struct.* **1995**, *356*, 49−62.
(19) Ishikawa, N.; Ohno, O.; Kaizu, Y.; Kobayashi, H. *J. Phys. Chem.* **1992**, *96*, 8832−8839.
(20) Langford, V. S. Ph.D. Dissertation, University of Canterbury, Christchurch, 1997.
(21) Langford, V. S.; Williamson, B. E. *J. Phys. Chem.* **1997**, *101*, 3119−3124.
(22) Stranger, R.; Dubicki, L.; Krausz, E. *Inorg. Chem.* **1996**, *35*, 4218−4266.
(23) Dunford, C. L.; Williamson, B. E. *J. Phys. Chem. A* **1997**, *101*, 2050−2054.
(24) Piepho, S. B.; Schatz, P. N. *Group Theory in Spectroscopy with Applications to Magnetic Circular Dichroism*; Wiley: New York, 1983.
(25) Stillman, M. J.; Nyokong, T. In *Phthalocyanines Properties and Applications*; Leznoff, C. C., Lever, A. B. P., Eds.; VCH Publishers: New York, 1989; Vol. II, pp 133−257.
(26) Huang, T. H.; Rieckhoff, K. E.; Volgt, E. M. *J. Chem. Phys.* **1981**, *85*, 3322−3326.
(27) VanCott, T. C.; Rose, J. L.; Williamson, B. E.; Boyle, M. E.; Misener, G. C.; Schrimpf, A. E.; Schatz, P. N. *J. Phys. Chem.* **1989**, *93*, 2999−3011.
(28) Canters, G. W. *J. Chem. Phys.* **1981**, *74*, 157−162.
(29) McClure, D. S. *J. Chem. Phys.* **1952**, *20*, 682−686.
(30) Ake, R. L.; Gouterman, M. *Theor. Chim. Acta* **1969**, *15*, 20−42.
(31) Altmann, S. L.; Herzig, P. *Point-Group Theory Tables*; Clarendon Press: Oxford, 1994.
(32) Wybourne, B. G. *Spectroscopic Properties of Rare Earths*; Interscience Publishers: New York, 1965.
(33) Dieke, G. H. *Spectra and Energy Levels of Rare Earth Ions in Crystals*; Interscience Publishers: New York, 1968.
(34) McClure, D. S. *Electronic Spectra of Molecules and Ions in Crystals*; Solid State Reprints; Academic Press: New York, 1959.